DMD Fast Forward. Published on July 21, 2011 as doi:10.1124/dmd.110.036848

Title page

CYP4F3B expression is associated with differentiation of HepaRG human hepatocytes and unaffected by fatty acid overload.

Stéphanie Madec, Virginie Cerec, Emmanuelle Plée-Gautier, Joseph Antoun, Denise Glaise, Jean-Pierre Salaun, Christiane Guguen-Guillouzo and Anne Corlu

CNRS, UMR 7139, Station Biologique, BP74, 29682 Roscoff Cedex, France. (S.M., J-P. S.)

Inserm, UMR–S 991, Liver Metabolisms and Cancer, Université de Rennes 1, CHU Rennes, avenue de la bataille Flandres-Dunkerque, 35033 Rennes, France. (V.C., D.G., C.G-G, A.C.)

Université de Bretagne Occidentale, Laboratoire de Biochimie, EA-948, Faculté de Médecine, CS 93837, 29238 Brest Cedex 3, France. (E. P-G., J.A., J-P. S)

DMD Fast Forward. Published on July 21, 2011 as DOI: 10.1124/dmd.110.036848
This article has not been copyedited and formatted. The final version may differ from this version.

Running title page

Running title: CYP4F3B and ω-hydroxylation of fatty acids in HepaRG cells

Corresponding authors: Dr C. Guguen-Guillouzo and Dr A. Corlu, INSERM UMR-S 991, Hôpital Pontchaillou, 35033 Rennes cedex (France), Tel +33 (0)2 23 23 38 52, Fax +33 (0)2 99 54 01 37, e-mails : christiane.guillouzo@univ-rennes1.fr, anne.corlu@inserm.fr

Number of text pages: 30

Number of tables: 4

Number of figures: 6

Number of references: 39

Numbers of words in the abstract: 241

Numbers of words in the introduction: 743

Numbers of words in the discussion: 1503

Abbreviations:

9,10-diHSTA, 9,10-dihydroxystearic acid; 9(10)-EpSTA, *Z*9(10)-epoxystearic acid or *Z*9(10)-epoxyoctadecanoic acid; 18-HEpSTA, 18-Hydroxy-9,10-epoxystearic acid; 9,10-diHSTA, BSTFA/TMCS: N,O-bis(trimethylsilyl)trifluoromethylacetamide with 1% trimethylchlorosilane; AA, arachidonic acid; ATCC, American type culture collection; CAR, constitutive androstane receptor; C/EBPα, CCAAT/enhancer binding protein alpha; CYP4F, Cytochromes P450 of the subfamily 4F; DHA, docosahexaenoic acid, DMSO, Dimethyl sulfoxide; EPA, eicosapentaenoic acid, EETs, epoxyeicosatrienoic acids; FA, fatty acid; FAS, Fatty acid synthase; GAPDH, Glyceraldehyde 3-phosphate dehydrogenase; GC-MS, Gas Chromatography-Mass Spectrometry; MUFA, monounsaturated acid, PBS, Phosphate buffered saline; PEPCK-1, Phosphoenolpyruvate carboxykinase 1; PPAR, Peroxisome Proliferator Activated Receptor; PUFA, Polyunsaturated Fatty Acid; PXR, pregnane X

receptor; RNA, Ribonucleic acid; RP-HPLC, Reverse Phase-High Performance Liquid Chromatography; SDS-PAGE, Sodium Dodecyl Sulfate-Polyacrylamide Gel Electrophoresis; SREBP-1c, Sterol Regulatory Element Binding Protein-1; TBS, Tris Borate Sulfate; TG, Triglycerides; VLDL, Very Low Density lipoprotein**.**

Abstract

Fatty acid microsomal ω-oxidation involves CYP450 enzymes. Some of them belonging to the CYP4F3 family are mainly expressed in the liver making this organ a major player in energy homeostasis and lipid metabolism. To study this important regulation pathway, we used HepaRG cells which gradually undergo a complete differentiation process. Even at the early stage of the differentiation process, CYP4F3B generated by alternative splicing of the CYP4F3 gene represented the prevalent isoform in HepaRG cells as in the liver. Its increasing expression associated with hepatocyte differentiation status suggested a hepatic-specific control of this isoform. As in liver microsomes, the catalytic hydroxylation of the CYP4F3B substrate [1-14C]Z9(10)-epoxystearic acid led to major production of 18-hydroxy-Z9(10)-epoxystearic acid. When treated with saturated, monounsaturated or polyunsaturated fatty acids, CYP4F3B and CYP4A11 expression remained unchanged while CYP4F2 and CYP4F12 expression were transiently up-regulated. A 24 hours exposure of differentiated HepaRG cells to various polyunsaturated fatty acids and derivatives induced microvesicular steatosis, down-regulation of lipid metabolism gene regulators such as SREBP-1c, FAS, PPARγ, PPARα and decreased expression of glucose-dependent metabolism genes which could limit *de novo* lipogenesis. Docosahexaenoic acid appeared to be the most effective compound. These results suggest that a PPARα independent pathway could participate to limit lipogenesis and emphasize the role of hepatocytes in fatty acids ω-hydroxylation pathway. They also give insights on the use of HepaRG hepatocytes to open new avenues of investigations on factors mediating the lipid metabolic pathway and finding new hypolipidemic molecules.

DMD Fast Forward. Published on July 21, 2011 as DOI: 10.1124/dmd.110.036848
This article has not been copyedited and formatted. The final version may differ from this version.

Introduction

Interest in lipid metabolism has greatly increased in the last decade because of its strong influence onto obesity leading to metabolic syndrome pathologies including vascular and liver disorders. Common to obesity-related dyslipidemia and hypertriglyceridemia is the excessive storage of fatty acids (FAs) in the liver (steatosis) frequently referred as nonalcoholic fatty liver disease (NAFLD). However, we are just beginning to understand how FAs induce oxidative stress and progression of steatosis to steatohepatitis characterized by inflammation processes (NASH). Associated alterations in glucose, FAs and lipoprotein metabolism may account for causal or responsive effectors to occurrence of these abnormalities (Fabbrini et al., 2010). Even if the major FA catabolism pathway is β-oxidation, there is a growing body of evidence that another way, the microsomal ω-oxidation mediated by CYP450 enzymes, plays a pivotal role in synthesis of lipids mediators, energy homeostasis and lipid accumulation (Hardwick et al., 2008). This latter pathway which mainly involves the CYP4A/4F subfamilies that preferentially hydroxylate the terminal methyl group of the FA chain (Sanders et al., 2006; Hsu et al, 2007), provides a novel route to eliminate the potential toxic levels of free FAs. Therefore, they may represent therapeutic targets and efforts in increasing our understanding of their regulation would be very helpful.

Among CYPs including CYP4A11, CYP4F2 and CYP4F3A/3B, the latter is the best known to ω-hydroxylate the essential FA arachidonate to 20-HETE, a potent vasoactive ecosanoid and anti-inflammatory agent (Kalsotra et al., 2006; Fer et al., 2008). The CYP4Fs are predominantly expressed in liver and kidney, although CYP4F3A is found in myeloid tissue. Different regulation for their tissue-dependent expression has been proposed. For instance, tissue-specific transcription factors such as the hepatocyte nuclear factor 4α (HNF4α) controls the expression of key genes involved in hepatic very-low-density lipoprotein (VLDL) metabolism (Petrescu et al., 2002). Alternative splicing is also increasingly recognized as a shared theme in CYP gene regulation to generate tissue-specific expression of CYPs (Nelson et al., 2004). A pertinent example is provided by the functionally distinct CYP4F3 isoforms which are regulated by alternative promoter usage and

DMD Fast Forward. Published on July 21, 2011 as DOI: 10.1124/dmd.110.036848
This article has not been copyedited and formatted. The final version may differ from this version.

mutually exclusive exon splicing (Christmas et al., 2001). Selection of exon 4 generates the CYP4F3A isoform which has a low K_m for leukotriene B4 (LTB4) and is mainly expressed in neutrophils. Meanwhile, selection of exon 3 generates an alternative isoform (CYP4F3B) which has 44 fold lower efficiency of inactivating LTB4, which is expressed in liver and has a preference for arachidonic acid (AA) as a substrate to convert it to 20-HETE. These contrasting abilities of the CYP4F3 isoforms allow versatility function but require strict controls which are still poorly documented.

In addition, expression of CYP4A/4F gene families can be highly modulated by various environmental factors, for instance fasting, high fat diet, hypolipidemic drugs or peroxisome proliferators (Hardwick, 2008, Hardwick et al., 2009) and by endogenous lipid mediator such as prostaglandin A1 (Antoun et al., 2008). Moreover, different intracellular types of FAs and their metabolites may coordinate energy homeostasis by activation or repression of distinct transcriptional factors including peroxisome proliferator activated receptors (PPARα, PPARβ, PPARγ), sterol regulatory element binding proteins (SREBP-1 and SREBP-2), liver X receptor (LXRα) suggesting involvement of distinct signalling pathways.

Studies on regulation processes of CYPs involved in these pathways have been hampered by the limited availability and the inherent variability of human liver material. In this study, the CYP4F3B expression has been analyzed in HepaRG cells and compared to two different human hepatoma-derived cell lines namely HepG2 and Huh-7 known to support several liver-specific functions. In contrast to the others, HepaRG cells display characteristics of hepatic progenitors i.e. high capacity for self-renewal and expression of numerous markers of early hepatic progenitors or oval cells (Cerec et al., 2007). Moreover, those cells directed towards the hepatocyte lineage at confluence, can undergo a gradual and complete hepatic differentiation program similar to normal hepatocytes with expression of a large panel of liver-specific genes including the major drug metabolizing enzymes (Aninat et al., 2006; Le Vee et al., 2006). Here, we showed that HepaRG cells expressed the tissue-specific CYP4F3B isoform and the CYP4A11 at higher levels than other hepatocellular cell lines and that their expression levels were strongly linked to the cell differentiation status. Moreover,

DMD Fast Forward. Published on July 21, 2011 as DOI: 10.1124/dmd.110.036848
This article has not been copyedited and formatted. The final version may differ from this version.

the CYP4F3B catalytic activity was similar to that observed in human liver microsomes and exposure of differentiated HepaRG cells to various FAs induced a hepatocyte steatosis and adaptive response which participated to reduce neolipogenesis. All together, our results showed that FAs metabolism in HepaRG hepatocytes is highly similar to human liver.

DMD Fast Forward. Published on July 21, 2011 as DOI: 10.1124/dmd.110.036848
This article has not been copyedited and formatted. The final version may differ from this version.

Materials and methods

Chemicals. Radiolabeled [1-^{14}C]*Z*9(10)-epoxystearic acid (57 Ci/mol) was from CEA (Gif sur Yvette, France). *Z*9(10)-epoxystearic acid, stearic acid, palmitic acid, oleic acid, linoleic acid, alpha-linolenic acid, eicosapentaenoic acid (EPA), docosahexaenoic acid (DHA) and arachidonic acid (AA) were obtained from Cayman Chemicals (SPI Bio, Massy, France). The silylating reagent, N,O-bistrimethylsilyltrifluoroacetamide (BSTFA) containing 1% of trimethylchlorosilane (TMCS) was obtained from Pierce Europe (Ound-Beijerland, The Netherlands). All chemicals and solvents were purchased from Merck (Darmstadt, Germany) and Sigma-Aldrich (Lyon, France).

Culture conditions.

The new cell line, HepaRG, established by Gripon et al. (2002) was maintained as previously described, in the growth medium composed of William's E medium (Invitrogen) supplemented with L- glutamine, 10% fetal calf serum (Hyclone), 5 µg/ml insulin (Sigma-Aldrich) and 5.10^{-5}M hydrocortisone hemisuccinate (Upjohn Pharmacia). Cells were seeded at the density of 2.6×10^4 cells/cm^2 and reached confluence in 4 days. After 15 days, they were maintained in the growth medium supplemented with 2% DMSO (Sigma-Aldrich) for 2 more weeks. The medium was renewed every 2 or 3 days. The HepG2 cell line and a derived clone C3A as well as the Huh-7 cell line were obtained from the ATCC Collection. They were maintained in the growth media recommended by ATCC and used after 7 days of confluence for Huh-7 and 3 weeks of culture for HepG2 cell lines.

To evaluate the effect of DMSO and the involvement of HNF4α on the CYP4F3B expression, differentiated HepaRG cells were cultured three days without DMSO before treatment. Then HepaRG cells were treated for either 18 hours with 0.1 or 2% of DMSO or 24h with 50,100 and 200 µM of linoleic acid.

For the FAs treatment, differentiated HepaRG cells were incubated with different saturated fatty acids, monounsaturated fatty acids (MUFAs) or polyunsaturated fatty acids (PUFAs) at concentration ranging from 50 to 200 µM (stearic acid, palmitic acid, oleic acid, linoleic acid,

DMD Fast Forward. Published on July 21, 2011 as DOI: 10.1124/dmd.110.036848
This article has not been copyedited and formatted. The final version may differ from this version.

alpha-linolenic acid, EPA, DHA and AA) for 6, 15 or 24h in a DMSO and fetal calf serum deprived medium supplemented with 1% of bovine serum albumin fraction V fatty acid free. In some experiment, a combination of palmitic/oleic acids with a ratio 1:1 was also used.

Peripheral blood mononuclear cells (PBMC) were isolated from healthy blood donor's buffy-coats by centrifugation on Ficoll-Hypaque gradient (GE Healthcare). Access to biopsy material was in agreement with French laws and satisfied the requirements of the Ethics Committee of the institution.

Incubation of HepaRG cells with Z9(10)-EpSTA.

Differentiated HepaRG cells were incubated with 20 µM of radiolabeled [1-^{14}C]*Z*9-(10)-epoxystearic acid (Z9(10)-EpSTA (Specific Activity 4 µCi/µmol), a discriminating substrate of CYP4F3 (Le Quéré et al, 2004) for 30 min at 37°C. 9-(10)-EpSTA was added in DMSO to 5 ml of culture medium. After incubation, medium and cells (2 ml PBS) were collected and stored at –80°C.

Isolation of total RNA, Northern blot and reverse transcription.

Total cell RNA was extracted by the Total SV RNA kit (Promega) or semi-automatic RNA extraction using the ABI Prism 6100 Nucleic Acid PrepStation. Concentration of each sample was spectrophotometrically determined and their integrity was confirmed using an Agilent 2100 Bioanalyser (Agilent Technologies, Palo Alto, CA). RNAs were fractionated on a 1.5% agarose gel and analysed by standard Northern blot procedure. Control of the RNA amount transferred onto filters was performed after methylene blue staining. Reverse transcription (RT) mixtures using high capacity cDNA kit (Applied biosystems) contained 50 µl of pure RNA samples. RT reaction proceeded for 10 minutes at 25°C, 2 hours at 37°C and cDNAs were then stored at –80°C.

DMD Fast Forward. Published on July 21, 2011 as DOI: 10.1124/dmd.110.036848
This article has not been copyedited and formatted. The final version may differ from this version.

Real-time RT-PCR.

Quantitative polymerase chain reaction (QPCR) was performed by real-time fluorescent PCR using the ABI PRISM™7000 sequence detection system (Applied Biosystems) and detection used a fluorescent dye (SYBR Green) according to the manufacturer recommendations. Primer pairs of transcript were either chosen with primers 3 software (http://frodo.wi.mit.edu/cgi-bin/primer3/primer3www.cgi) (Table 1) or purchased from Applied Biosystems (PEPCK1, Hs00159918_m1*, CYP4A11, Hs04194779_g1*, GAPDH hs02758991_g1*). Reactions were carried out with 10-20 ng cDNAs. Three-step thermocycling was performed for 40 cycles. To normalise the amount of total RNA present in each reaction, we amplified the housekeeping gene glyceraldehyde-3-phosphate dehydrogenase (GAPDH). PCR amplifications were done in triplicates for each sample.

Microsomal preparation from tissue and cell culture.

Human biopsies were obtained from adult donors undergoing resection for primary and secondary tumors. Microsomes from human livers and HepaRG cells were prepared after homogenization of the tissues or cells as previously described (Berthou et al., 1989).

Western blot.

Microsomal proteins (1-5 µg) were resolved on 9% SDS-PAGE, transferred onto nitrocellulose membrane and blotted overnight at 4°C with a rabbit polyclonal antibody anti-CYP4F2 (RDI, Flanders NJ, US) cross reacting with CYP4F3A, CYP4F3B and CYP4F12 but not with CYP4A11. Specific protein expression was compared to the spot obtained with human recombinant CYP4F3B-containing insect cell microsomes (Supersomes™, Gentest, Woburn, MA) and human liver biopsy microsomes (ECL, GE Healthcare). Densitometry analysis was performed using BIO1D scanning software (Vilber Lourmat, France).

Proteins (50 µg) from HepaRG cells were resolved on 4-12% gradient SDS-PAGE, transferred onto nitrocellulose and blotted with either CYP4F3B-specific anti-peptide antibody raised against the amino acids encoded by the CYP4F3B-specific exon (position 232-374

DMD Fast Forward. Published on July 21, 2011 as DOI: 10.1124/dmd.110.036848
This article has not been copyedited and formatted. The final version may differ from this version.

from sequence AF05482 as described previously (Antoun et al., 2008) (Eurogentec, Seraing, Belgium) or a rabbit anti-CYP4A11 primary polyclonal antibody (RDI, Flanders, United State, ref:RDI, -CYP4A11abr). After washing with PBS, they were treated with PBS containing anti-rabbit Ig-biotinylated species-specific secondary antibody conjugated to streptavidine-horseradish peroxidase and then washed with PBS. The peroxidase activities were evidenced by ECL detection using luminol.

Immunochemical analysis and Oil-red O staining.

Cells were fixed with 4% paraformaldehyde for 20 minutes at 4°C. Incubation with primary antibody directed against albumin (Kent Laboratories), CYP3A4 (Chemicon® international) was performed at 4°C overnight and then, with the peroxidase-conjugated secondary antibody (Jackson laboratories) for 1 hour. Peroxidase staining was obtained with 3, 3'-diaminobenzidin/H_2O_2 solution and counterstaining with Masson's Hemalum. Intracellular neutral lipid deposition was stained by Oil-red O. Briefly, the cells were washed with ice-cold PBS twice, fixed with 4% paraformaldehyde at 4°C for 1 h, and stained with 0.2% Oil red O in isopropanol for 10 min. The cells were then washed with 70% ethanol and water.

Lipid extraction.

Radioactivity was quantified in 100 µl fractions from both medium and cell pellet. The medium and cell pellets were divided in two equal fractions, lyophilized and either dissolved in 100 µl of methanol or added to 500 µl of acetate buffer pH 5.2 containing 20 µl of helixpomacia suc for selective hydrolysis of glucuronoconjugated metabolites. After overnight incubation at 37°C and extraction with ethylacetate, compounds were dissolved in 50 µl of ethanol and analyzed by RP-HPLC.

RP-HPLC and GC-MS analyses of metabolites.

The oxidized metabolites and residual substrates were separated by RP-HPLC using a 5 µm Ultrasphere C18 column 150x4.6 mm (Beckman) using a mobile phase constituted of a

mixture of water and acetonitrile (71:29 v/v) containing 0.2% of acetic acid at a flow rate of 2 ml/min for 35 minutes. The residual substrates were eluted by applying a mixture of water/acetonitrile (5:95 v/v) containing 0.2% acetic acid for 5 minutes. The radioactivity of RP-HPLC effluent was monitored with a computerized on-line scintillation counter (Flo-one Beta Radiometric detector, Packard). The rate of radiolabeled metabolites generated was calculated from peak areas.

GC-MS analysis (E.I., 70 eV) was carried out on a gas chromatograph (HP 5890 Series II; Agilent Technology) equipped with a fused silica capillary column (HP-5MS 5% phenyl methyl siloxane; 30 m x0.32 mm i.d., 0.25 µm thick film) as previously described (Le Quéré et al., 2004). Mass spectra of Me/TMS derivatives contained in peaks with retention time of 21.2 and 26.5 min showed typical fragment ions at m/z = 73, 113, 155, 215, 259 and 443 (M^+-31) corresponding to 9,10-dihydroxyoctadecanoic acid (Fig 3, peak 2) and m/z = 73, 103, 155, 199, 215, 243, 385 (M^+-15) corresponding to 18-hydroxy-9,10-epoxyoctadecanoic acid (Fig 3, peak 5) respectively.

Statistical analyses

Data were expressed as means ± SD. Statistical analyses were performed using the nonparametric Mann-Whitney U test. Values of $p \leq 0.05$ were accepted as significant.

DMD Fast Forward. Published on July 21, 2011 as DOI: 10.1124/dmd.110.036848
This article has not been copyedited and formatted. The final version may differ from this version.

Results

Morphological and functional characteristics associated to the HepaRG cell differentiation program

Just after seeding, HepaRG cells appeared as a homogeneous cell population with elongated shape characteristic of progenitor cells (Fig. 1A). When maintained in the growth medium for 2 weeks followed by 2 additional weeks in the same medium supplemented with 2% DMSO, an active differentiation program was observed and schematically divided in 4 steps: elongated cells actively dividing up to reach confluence within 4-5 days (step 1) (Fig. 1B); occurrence of colonies of granular cells which gradually got the appearance of hepatocyte-like cells at confluence in one week (step 2); cords of cells exhibiting, typical hepatocyte-like phenotype surrounded by flat sheets of clear epithelial cells after 2 weeks (step 3) (Fig. 1C). The 4th stage covering the period of DMSO exposure is associated with increased hepatocyte-like cell colonies with high polarity as evidenced by the appearance of numerous bile canaliculus-like structures (arrow, Fig. 1D).

In parallel, from step 2, hepatocyte-like colonies, but not the surrounding biliary cells expressed sets of liver-specific functions, among them plasma proteins such as transferrin and albumin (arrow, Fig. 1E), glycolytic enzymes such as aldolase B and detoxication enzymes such as CYP4A11 and CYP3A4 (arrow, Fig. 1F). Comparison of mRNA kinetics of these specific functions showed that the specific glycolytic enzyme expression occurred much earlier than the detoxication enzyme CYP3A4, the latter being preceded by the liver-specific transcription factor HNF4α which clearly occurred at day 10. Expression of all these genes gradually increased thereafter (Fig. 1G), thus characterizing the differentiation steps of HepaRG hepatocytes.

CYP4F3B gene expression is strongly associated with the hepatocyte differentiation process in HepaRG cells

CYP4F3 gene expression was measured during the hepatic differentiation process and compared to other differentiation markers. As shown in table 2, the highest expression for

DMD Fast Forward. Published on July 21, 2011 as DOI: 10.1124/dmd.110.036848
This article has not been copyedited and formatted. The final version may differ from this version.

CYP4F3 was found in differentiated hepatocytes from step 3, with a gradual increase during the differentiation process similar to CYP3A4 and HNF4α expression profiles. Aldolase B accumulated at an earlier stage (step 2) while C/EBPα expression remained unchanged throughout the process. From day 15, HepaRG cells were exposed to 2% DMSO resulting within 10 days in dramatic increased levels of CYP4F3 (3-4 fold, step 4) as well as CYP3A4 (20-fold) and HNF4α (2-fold). To determine the contribution of DMSO "per se" added to the culture medium as an inducer of CYP4F3 expression differentiated HepaRG cells were exposed to increasing concentrations of DMSO up to 2% for 18 hours. A 5- to 6.4-fold induction with 1% and 2% DMSO respectively was found. Western blot analysis showed an accumulation of this enzyme in differentiated HepaRG cells (step 4) at a level close (70%) to that found in a human liver tissue (Fig 2A and 2B). This expression level was 10-fold higher than in HepG2 cells and at least twice as high as in HepG2/C3A and Huh-7 cells (Fig 2C).

To investigate which CYP4F isoform was predominantly expressed in HepaRG cells, we used two sets of primers especially designed to selectively amplify CYP4F3A and CYP4F3B mRNA isoforms. Considering expression in white blood cells arbitrary set at one, CYP4F3B mRNA expression appeared to be by far the predominant isoform in the liver and fully differentiated HepaRG cells (Table 3). As HNF4α is a key regulator of liver specific gene expression, HepaRG cells were exposed to one of its ligand, the linoleic acid, for 24h to study the effect on CYP4F3B and CYP3A4 expression (Yuan et al., 2009). While CYP3A4 expression, one of HNF4α target gene, increased, CYP4F3B expression remained unchanged (Fig. 2E). CYP4F3B expression profile during the differentiation process was then compared to other key genes involved in the regulation of the lipid metabolism (Table 4 and Fig 2D). Both CYP4A11 and PPARα exhibited a similar profile to CYP4F3B throughout the hepatocyte differentiation process while both PPARγ and SREBP-1c expression slightly increased up to the confluence stage but were poorly related to the hepatic differentiation process (step 3*).*

DMD Fast Forward. Published on July 21, 2011 as DOI: 10.1124/dmd.110.036848
This article has not been copyedited and formatted. The final version may differ from this version.

Metabolism of *Z*9(10)-epoxystearic acid by CYP4F3B in HepaRG cells

The catalytic functionality of CYP4F3B was assessed by incubating for 30 min differentiated HepaRG cells with [1-^{14}C]*Z*9(10)-EpSTA, a discriminating CYP4F3B substrate (Le Quéré et al., 2004). Measurement of the residual radioactivity of the medium and the cell pellet showed a disappearance of more than 30% of the starting radioactivity suggesting an efficient decarboxylation of the substrate probably by beta-oxidation. Analysis of the culture medium and the cell pellet before (Fig. 3, A and C) and after (Fig. 3, B and D) treatment with *Helixpomacia* suc suggested the presence of glucuronoconjugates (Fig. 3, A and C, peak 1) and showed the presence of 9,10-dihydroxystearic acid (9,10-diHSTA, Fig.3 B and D, peak 2) and unidentified metabolites. On the other hand, RP-HPLC (Fig. 3) demonstrated the ω-hydroxylation of *Z*9(10)-epoxystearic acid (9(10)-EpSTA) to 18-Hydroxy-9,10-epoxystearic acid (18-HEpSTA, Fig. 3D, peak 5) evidencing the involvement of CYP4F3B in the reaction. Moreover, incubation of microsomes from human liver (Fig. 3E) and differentiated HepaRG cells (Fig. 3F) with [1-^{14}C]9(10)-EpSTA was performed. Interestingly, the same RP-HPLC profile of radiolabeled metabolites was observed in both extracts: 9,10-diHSTA (peak 2), 18-HEpSTA (peak 5) and low amount of 9,10,18-trihydroxystearic acid (peak 4) were generated. Noteworthy this RP-HPLC profile was similar to that previously obtained after incubation of human liver microsomes with *Z*9(10)-EpSTA (Le Quéré et al., 2004). The chemical structure of these metabolites was confirmed by GC-MS analysis (not shown).

Influence of saturated FAs, MUFAs and PUFAs on CYPs expression in HepaRG cells

Hepatic expression of CYP4F and 4A genes can be induced by a number of different compounds such as FAs. To determine whether saturated, monounsaturated (MUFAs) or polyunsaturated fatty acids (PUFAs) can modulate CYP hydroxylases expression, we exposed for 6h, 15h and 24h differentiated HepaRG cells to increasing concentrations of stearic acid (C18:0), palmitic acid (C16:0), oleic acid (C18:1, ω–9), linoleic acid (C18:2, ω-6) as well as to a combination of palmitic/oleic acids which simulates dietary intake (Fig.4). Regardless of the fatty acid concentrations ranging from 50 to 200 µM or the duration of

DMD Fast Forward. Published on July 21, 2011 as DOI: 10.1124/dmd.110.036848
This article has not been copyedited and formatted. The final version may differ from this version.

treatment, no significant changes in CYP4F3B and CYP4A11 expression were detected. CYP4F2 and 4F12 expressions were only transiently up-regulated 6h after the FA treatment. Noteworthy, these inductions were not observed in cells treated with palmitic/oleic acid mixtures. In parallel, during the 6 to 15h treatment period, PPARα expression remained stable in all conditions before decreasing after 24h of treatment (Fig. 6 and not shown) suggesting at that time a modulation of the lipid metabolism.

Influence of different MUFAS and PUFAs on lipid metabolism regulator genes in HepaRG cells

In order to link HepaRG CYPs catalytic activity to lipid metabolism, we exposed differentiated HepaRG cells to six distinct PUFAs: oleic acid (C18:1, ω–9), linoleic acid (C18:2, ω-6), alpha-linolenic acid (C18:3, ω-3) and its 2 derivatives, eicosapentaenoic acid (EPA, C20:5, ω-3) and docosahexaenoic acid (DHA, C22:6, ω-3), and arachidonic acid (AA, C20:4, ω–6) for 24 hours, and steatosis was evaluated. Twenty four hours post FA treatments microvesicular steatosis characterized by accumulation of lipid droplets was assessed by Oil-red O staining (Fig. 5). Steatosis occurred in hepatocyte colonies and was triggered by all the different treatments. EPA and DHA gave the greatest lipid accumulation. In parallel, expression levels of lipid metabolism regulator genes (SREBP-1c, FAS, PPARα, PPARγ) were determined and compared to glucose metabolism enzymes (aldolase B and PEPCK-1) and to haptoglobin, an acute phase protein (Fig. 6). In the presence of all PUFAs tested, lipogenic gene expressions were all repressed while CYP4F3B and CYP4A11 (not shown) expression remained unchanged. Haptoglobin RNA levels were poorly modulated except with DHA which induced a dramatic inhibition of its expression. Interestingly PPARα expression, expected to be up-regulated, was down-regulated with a maximum inhibition also observed with DHA (up to 3-fold). Aldolase B glycolytic enzyme expression was clearly repressed by all PUFAs while the neoglucogenic enzyme, PEPCK-1 expression was only drastically reduced by DHA.

DMD Fast Forward. Published on July 21, 2011 as DOI: 10.1124/dmd.110.036848
This article has not been copyedited and formatted. The final version may differ from this version.

Discussion

Since the liver is the main source of major CYP-enzymes, it appears as the organ playing a central role in pathologies linked to obesity like cardiovascular and hepatic diseases both as victim and culprit (Goetzl et al., 1995). Indeed, by their typical common reactions to metabolize various substrates, CYP enzymes contribute to xenobiotic transformation, alcohol detoxication and lipid oxidation. ω-hydroxylation of both pro-and anti-inflammatory leukotrienes by members of the CYP4F subfamily directly contributes to the activation and resolution phases of the inflammatory response (Kikuta et al., 1994). As demonstrated in a previous work, CYP4F3 is the major CYP isoform catalyzing the ω-oxidation of AA and EETs derivatives in the human liver (Le Quéré et al., 2004).

Until now, studies on fatty acid metabolism and its regulations by the CYPs have been hampered by the absence of relevant in vitro models mimicking the human liver. Here, we demonstrated that the expression level of the CYP4F3B isoform was similar in HepaRG cells and in human liver microsomes and 10 and 3 times higher than in HepG2 and Huh-7 cells respectively. CYP4A11 was also highly expressed in HepaRG when compared to HepG2 and Huh-7 cells. Interestingly, CYP4F3B and CYP4A11 expressions were strictly associated with the differentiation process of HepaRG cells which was characterized by a gradual increased expression up to hepatocyte maturation of HNF4α, a well-known master regulator of hepatic specific genes, specific enzymes of glucose metabolism such as aldolase B, and CYP-enzyme families involved in phase 1 detoxication metabolism such as CYP3A4. These results strongly raise the question of its tissue-specific regulation.

Localization of CYP4F3 was thought to be restricted to myeloid cells until tissue-specific expression of one functionally distinct isoform, CYP4F3B, was discovered in the liver (Christmas et al., 2001). CYP4F3A and CYP4F3B were both expressed in the fetal liver but it was suggested that CYP4F3A was associated with its transient hematopoietic function. This study supports our observation that CYP4F3A was very weakly expressed in HepaRG cells regardless of their differentiation status, thus excluding the possibility of a balanced expression between the two isoforms in hepatic cells. This also confirms this alternative

splicing as a tissue-specific regulation (Christmas et al., 2001) and supports that its control could take place during the early stage of hepatic organogenesis.

CYP4F3B expression during hepatocyte differentiation matched that of HNF4α, CYP3A4 and CYP4A11 suggesting that various CYPs might share common mechanisms controlling gene expressions mediated by liver-specific transcription factors and nuclear receptors. HNF4α modulates the expression of a large number of genes involved in the uptake of lipoproteins, synthesis of cholesterol as well as triglycerides and VLDL processing (Hwang-Verslues and Sladek, 2010). A potential binding site for HNF4α was identified in the CYP4F3B isoform promoter in HepG2 cells (Christmas et al., 2003). Although CYP4F3B and CYP3A4 were expressed once HepaRG cells express HNF4α, we did not observe correlation between HNF4α activation and the regulation of CYP4F3B expression. However, we did observe an increase in CYP3A4 expression, one of well-known HNF4α target gene following linoleic acid exposure, identified as a reversible endogenous ligand for HNF4α (Yuan et al 2009).

It is now well established that DMSO potentiates hepatocyte differentiation (Isom et al., 1985, Gripon et al., 2002). DMSO exposure was found to greatly enhance the expression of several CYP isoforms and transporters in HepaRG cells (Aninat et al., 2006). Expression of both CYP4F3B and CYP3A4 was up-regulated by 6 and 15 fold respectively in HepaRG cells when treated with 2% DMSO while CYP4F3A remained barely expressed. Therefore, in agreement with Dickins (2004), our results led us to hypothesize that CYP3A4 and CYP4F3B could be regulated by a common mechanism involving one or several nuclear receptors such as RXR, PXR and CAR. Lambert et al., (2009) showed that phenobarbital, an activator of CAR and PXR, enhanced CYP4F3B but repressed CYP4A11. Similarly, we observed that CYP4A11 expression was down regulated in DMSO treated cells. This supports the well-established differential regulation of the human CYP4A genes, especially CYP4A11 which was shown to be regulated by retinoic acid, bezafibrate and dexamethasone in human (Antoun et al., 2006, Savas et al., 2003).

One of our major observations was related to the CYP4F3B catalytic activity in HepaRG cells. CYP4F3B from human liver microsomes was described as the major CYP isoform involved in the ω-hydroxylation of FA epoxides with unsaturated C18 and C20 carbon chains (Le Quéré et al., 2004). We showed that the oxidative metabolism of 9(10)-epoxystearic acid, a discriminating CYP4F3B substrate, was identical in HepaRG cells and in human liver microsomes. This confirmed that HepaRG cells preserved the ability to metabolize C18 epoxides with high efficiency via the same pathways as in the liver (Capdevila et al., 1988). Noteworthy, CYP4F3B was also identified as the enzyme producing 20-HETE in HepaRG cells (Antoun et al., 2008). This functional feature of HepaRG cells offers new clues to highlight the mechanisms of toxicity induced by FA derivatives described as toxic metabolites in mammals (Zheng et al., 2001,) but also by EETs, found to accumulate in alcoholic liver disease in rat (French et al., 1997).

Finally, we exposed differentiated HepaRG cells to different saturated FAs, MUFAs and/or PUFAs to compare the regulation of CYP4F3B expression to other CYPs involved in the lipid hydroxylation. No major modulation of the main CYP hydroxylase expression was detected except for a transient up-regulation of CYP4F2 and CYP4F12. Of note, induction of both CYP occurring 6h after treatment was absent when a combination of palmitic/oleic acids was used, suggesting that a mixture of saturated FAs and MUFAs alter the cellular metabolism profile during steatosis. A previous study highlighted differences in CYP4F2 and CYP4F3 gene promoter regions and showed that saturated FAs induced CYP4F2 expression in HepG2 cells (Zhang et al., 2000). Here, we demonstrated that CYP4F2 expression could also be up-regulated by MUFAs and PUFAs. Although, CYP4F12 was proved to be about 10 and 50 less efficient that CYP4A11 and CYP4F2 regarding FA hydroxylation, few data are available on its regulation. Like CYP4F2, we showed that CYP4F12 expression could be regulated by saturated or unsaturated FAs. Regarding CYP4A11 expression, it has been described that PPARα contributes to its basal expression and induction during fasting in mice (Savas et al., 2009). However, in human the CYP4A11 and CYP4F2 are not induced by peroxisome proliferators. In our experimental conditions, despite the fact that one cannot

DMD Fast Forward. Published on July 21, 2011 as DOI: 10.1124/dmd.110.036848
This article has not been copyedited and formatted. The final version may differ from this version.

exclude that CYP4A11 expression might decrease after 24h treatment, CYP4A11 and PPARα expression did not appear to be correlated; while PPARα expression decreased at 24h, CYP4A11 expression remained stable.

All saturated (not shown) and ω-3, ω-6 and ω-9 FAs induced a typical microvesicular steatosis evidenced by an accumulation of lipid droplets in hepatocytes after 24h treatment. The greatest effect was observed when HepaRG cells were treated with DHA and AA. CYP4F3B expression remained unchanged and maintained at a high level independently of the type of treatment. Meanwhile, a coordinated down-regulation of different regulator genes of lipid metabolism involved in the *de novo* hepatic lipogenesis was observed. Indeed, SREBP1-c, FAS and PPARγ expressions were down-regulated along with the expression of glycolytic and neoglucogenic enzymes leading to a limited carbon source for FA synthesis. All the effects were mainly observed following DHA treatment. Lipid accumulation in immortalized human hepatocytes was also reported to be associated with decreased lipogenesis (De Gottardi A et al., 2007). Regarding SREBPs, ω-3 PUFAs was found to reduce SREBP1-c activity when fed in the diet or incubated with HepG2 hepatoma cells (Ou et al., 2001).

The molecular regulations of hepatic gene expression via PUFAs are complex and most probably involve several mechanisms. Previous studies showed that both PPARα-dependent and -independent pathways occur in the liver (Ren et al., 1997). Interestingly, PPARα was inhibited in HepaRG cells despite the accumulation of PUFAs which is usually responsible for its activation (Hardwick et al., 2009). A hepatic refractoriness to activate PPARα has been well documented in metabolic syndrome-associated steatohepatitis (Larter et al., 2010). PPARα mRNA expression was also found down-regulated in hepatocytes after chylomicron remnant particules treatment (CMR). Noteworthy, CMR enriched in n-3 PUFAs appeared to be more potent than those rich in n-6 PUFAs (Zheng et al., 2002). In agreement with the latter observation, we found an important inhibition of PPARα following exposure to DHA reported as a major substrate for CYP4F2 and CYP4F3B and a powerful hypolipidemic compound (Kris-Etherton et al., 2002). Mater et al., (1999) suggested that the regulation of

lipogenic genes through PUFAs could involve PPARα-independent ways. In our experimental setting, transient activation of CYP4F2 and CYP4F12 by saturated and unsaturated FAs in human hepatic cells might contribute to the fine tuning of hepatic lipid metabolism.

Altogether, our results showed many similarities between HepaRG hepatocytes and hepatocytes *in vivo* regarding CYP4F3B-mediated FA metabolism and demonstrated the value of the stepped-up hepatic differentiation to understand specific gene regulation. This cellular model opens new experimental avenues to improve our knowledge in factors mediating lipid metabolic pathways and their regulation by environmental conditions. This would also greatly help screening agonist and antagonist molecules for therapeutic, preventive or curative purposes for liver diseases related to lipid metabolic disorders.

Acknowledgements

We thank Drs. André Guillouzo and Bernard Fromenty for helpful comments and critical reading of the article and the Biological Resource Center of Rennes for supply of human hepatic samples.

Authorship contributions

Participated in research design: Madec, Cerec, Plée-Gautier, Antoun, Corlu, Salaun and Guguen-Guillouzo.

Conducted experiments: Madec, Cerec, Glaise and Antoun.

Contributed new reagents or analytical tools:

Performed data analysis: Madec, Cerec, Antoun, Salaun, Plée-Gautier, Corlu and Guguen-Guillouzo.

Wrote or contributed to the writing of the manuscript: Madec, Cerec, Guguen-Guillouzo and Corlu.

References

Aninat C, Piton A, Glaise D, Le Charpentier T, Langouët S, Morel F, Guguen-Guillouzo C, and Guillouzo A (2006) Expression of cytochromes P450, conjugating enzymes and nuclear receptors in human hepatoma HepaRG cells. *Drug Metab Dispos* **34**:75-83.

Antoun J, Amet Y, Simon B, Dréano Y, Corlu A, Corcos L, Salaun JP, and Plée-Gautier E (2006) CYP4A11 is repressed by retinoic acid in human liver cells. *FEBS Letters* **580**:3361-3367.

Antoun J, Goulitquer S, Amet Y, Dreano Y, Salaun JP, Corcos L, and Plée-Gautier E (2008) CYP4F3B is induced by PGA1 in human liver cells: a regulation of the 20-HETE synthesis. *J Lipid Res* **49**:2135-2141.

Berthou F, Ratanasavanh D, Riche C, Picart D, Voirin T, and Guillouzo A (1989) Comparison of caffeine metabolism by slices, microsomes and hepatocyte cultures from adult human liver. *Xenobiotica* **19**:401–417.

Capdevila JH, Mosset P, Yadagiri P, Lumin S, and Falck JR (1988) NADPH-dependent microsomal metabolism of 14,15-epoxyeicosatrienoic acid to diepoxides and epoxyalcohols. *Arch Biochem Biophys* **261**:122-133.

Cerec V, Glaise D, Garnier D, Morosan S, Turlin B, Drenou B, Gripon P, Kremsdorf D, Guguen-Guillouzo C, and Corlu A (2007) Transdifferentiation of hepatocyte-like cells from the human hepatoma HepaRG cell line through bipotent progenitor. *Hepatology* **45**:957-967.

Christmas P, Jones JP, Patten CJ, Rock DA, Zheng Y, Cheng SM, Weber BM, Carlesso N, Scadden DT, Rettie AE, and Soberman RJ (2001) Alternative splicing determines the function of CYP4F3 by switching substrate specificity. *J Biol Chem* **276**:38166-38172.

Christmas P, Carlesso N, Shang H, Cheng SM, Weber BM, Preffer FI, Scadden DT, and Soberman RJ (2003) Myeloid expression of cytochrome P450 4F3 is determined by a lineage-specific alternative promoter.*J Biol Chem* **278**:25133-142.

De Gottardi A, Vinciguerra M, Sgroi A, Moukil M, Ravier-Dall'Antonia F, Pazienza V, Pugnale P, Foti M, and Hadengue A (2007) Microarray analyses and molecular profiling of steatosis induction in immortalized human hepatocytes. *Lab. Invest* **87**:792-806.

Dickins M (2004) Induction of cytochromes P450. *Curr Top Med Chem* **4**:1745-66.

Fabbrini E, Sullivan S, and Klein S (2010) Obesity and nonalcoholic fatty liver disease: biochemical, metabolic, and clinical implications. *Hepatology* **51**:679-689.

Fer M, Corcos L, Dréano Y, Plée-Gautier E, Salaun JP, Berthou F, and Amet Y (2008) Cytochrome P450 from family 4 are the main omega hydroxylating enzymes in humans: CYP4F3B is the prominent player in PUFA metabolism. *J Lipid Res* **49**:2379-2389.

French SW, Morimoto M, Reitz RC, Koop D, Klopfenstein B, Estes K, Clot P, Ingelman-Sundberg M, and Albano E (1997) Lipid peroxidation, CYP2E1 and arachidonic acid metabolism in alcoholic liver disease in rats. *J Nutr* **127**:907S-911S.

Goetzl EJ and An S, and Smith WL (1995) Specificity of expression and effects of eicosanoid mediators in normal physiology and human diseases. *Faseb J* **9**:1051-1058.

Gripon P, Rumin S, Urban S, Le Seyec J, Glaise D, Cannie I, Guyomard C, Lucas J, Trepo C, and Guguen-Guillouzo C (2002) Infection of a human hepatoma cell line by hepatitis B virus. *Proc Natl Acad Sci USA* **99**:15655-15660.

Hardwick JP (2008) Cytochrome P450 omega hydroxylase (CYP4) function in fatty acid metabolism and metabolic diseases. *Biochem Pharmacol* **75**:2263-2275.

Hardwick JP, Osei-Hyiaman D, Wiland H, Abdelmegeed MA, and Song BJ (2009) PPAR/RXR Regulation of Fatty Acid Metabolism and Fatty Acid omega-Hydroxylase (CYP4)

Isozymes: Implications for Prevention of Lipotoxicity in Fatty Liver Disease. *PPAR Res* **2009**:952734.

Hsu MH, Savas U, Griffin KJ, and Johnson EF (2007) Human cytochrome p450 family 4 enzymes: function, genetic variation and regulation. *Drug Metab Rev* **39**:515-538.

Hwang-Verslues WW, and Sladek FM (2010) HNF4α - role in drug metabolism and potential dug target? *Curr Opin Pharmacol* **10**:698-705.

Isom HC, Secott T, Georgoff I, Woodworth C, and Mummaw J (1985) Maintenance of differentiated rat hepatocytes in primary culture. *Proc Natl Acad Sci USA* **82**:3252-3256.

Kalsotra A and Strobel HW (2006) Cytochrome P450 4F subfamily: At the crossroads of ecosanoid and drug metabolism. *Pharmacol Ther* **112**:589-611.

Kikuta Y, Kusunose E, Kondo T, Yamamoto S, Kinoshita H, and Kusunose M (1994) Cloning and expression of a novel form of leukotriene B4 omega-hydroxylase from human liver. *FEBS Lett* **348**:70-74.Kris-Etherton PM, Harris WS, and Appel LJ (2002) Fish consumption, fish oil, omega-3 fatty acids, and cardiovascular disease. *Circulation* **106**:2747-2757.

Lambert CB, Spire C, Claude N, and Guillouzo A (2009) Dose- and time-dependent effects of phenobarbital on gene expression profiling in human hepatoma HepaRG cells. *Toxicol Appl Pharmacol* **234**:345-360.

Larter CZ, Chitturi S, Heydet D, and Farrell GC (2010) A fresh look at NASH pathogenesis. Part 1: the metabolic movers. *J Gastroenterol Hepatol* 2**5**:672-690.

Le Quéré V, Plee-Gautier E, Potin P, Madec S, and Salaun JP (2004) Human CYP4F3s are the main catalysts in the oxidation of fatty acid epoxides. *J Lipid Res* **45**:1446-1458.

Le Vee M, Jigorel E, Glaise D, Gripon P, Guguen-Guillouzo C, and Fardel O (2006) Functional expression of sinusoidal and canalicular hepatic drug transporters in the differentiated human hepatoma HepaRG cell line. *Eur J Pharm Sci* **28**:109-117.

Mater MK, Thelen AP, Pan DA, and Jump DB (1999) Sterol response element-binding protein 1c (SREBP-1c) is involved in the polyunsaturated fatty acid suppression of hepatic S14 gene transcription. *J Biol Chem* **274**:32725-32732.

Nelson DR, Zeldin DC, Hoffman SM, Maltais LJ, Wain HM, and Nebert DW (2004) Comparison of cytochrome P450 (CYP) genes from the mouse and human genomes, including nomenclature recommendations for genes, pseudogenes and alternative-splice variants. *Pharmacogenetics* **14**:1-18.

Ou J, Tu H, Shan B, Luk A, DeBose-Boyd RA, Bashmakov Y, Goldstein JL, and Brown MS (2001) Unsaturated fatty acids inhibit transcription of the sterol regulatory element-binding protein-1c (SREBP-1c) gene by antagonizing ligand-dependent activation of the LXR. *Proc Natl Acad Sci U S A* **98**:6027-6032.

Petrescu AD, Hertz R, Bar-Tana J, Schroeder F, and Kier AB (2002) Ligand specificity and conformational dependence of the hepatic nuclear factor-4alpha (HNF-4alpha). *J Biol Chem* **277**:23988-23999.

Ren B, Thelen AP, Peters JM, Gonzalez FJ, and Jump DB (1997) Polyunsaturated fatty acid suppression of hepatic fatty acid synthase and S14 gene expression does not require peroxysome proliferator-activated receptor α. *J Biol Chem* **272**:26827-26832.

Sanders RJ, Ofman R, Duran M, Kemp S, and Wanders RJ (2006) Omega-oxidation of very long-chain fatty acids in human liver microsomes. Implications for X-linked adrenoleukodystrophy. *J Biol Chem* **281**: 13180-13187.

Savas U, Hsu MH, and Johnson EF (2003) Differential regulation of human CYP4A genes by peroxisome proliferators and dexamethasone. *Arch Biochem Biophys* **409**:212-20.

Savas U, Machemer DE, Hsu MH, Gaynor P, Lasker JM, Tukey RH, and Johnson EF(2009) Opposing roles of peroxisome proliferator-activated receptor alpha and growth hormone in the regulation of CYP4A11 expression in a transgenic mouse model. *J Biol Chem*. **284**:16541-52.

Yuan X, Ta TC, Lin M, Evans JR, Dong Y, Bolotin E, Sherman MA, Forman BM, and Sladek FM (2009) Identification of an endogenous ligand bound to a native orphan nuclear receptor. *PLoS One*. **4**:e5609

Zhang X, Chen L, and Hardwick JP (2000) Promoter activity and regulation of the CYP4F2 leukotriene B(4) omega-hydroxylase gene by peroxisomal proliferators and retinoic acid in HepG2 cells. Arch *Biochem Biophys*. **378**:364-376

Zheng J, Plopper CG, Lakritz J, Storms DH, and Hammock BD (2001) Leukotoxin-diol: a putative toxic mediator involved in acute respiratory distress syndrome. *Am J Respir Cell Mol Biol* **25**:434-438.

Zheng X, Rivabene R, Cavallari C, Napolitano M, Avella M, Bravo E, and Botham KM (2002) The effects of chylomicron remnants enriched in n-3 or n-6 polyunsaturated fatty acids on the transcription of genes regulating their uptake and metabolism by the liver: influence of cellular oxidative state. *Free Radic Biol Med* **32**:1123-1131.

Footnotes

This work was supported by l'Agence nationale de la recherche [grant PCV07_184566 µHepaReTox project] ; le Conseil Régional de Bretagne [grant PRIR-A3CBL9; N°560408] ; the European Community 6th Framework Program [grant COMICS project N° 037575]. This research was also supported in part by Institut National de la Santé et Recherche Médicale ; Centre National de Recherche Scientifique et Technique. S.M. was recipient of ANRT fellowship, V.C was recipient of ANRT and BIOPREDIC International Company fellowship.

[1] Stéphanie Madec

[2] Virginie Cerec

[3] Emmanuelle Plée-Gautier

[4] Joseph Antoun

[5] Denise Glaise

[6] Jean-Pierre Salaun

[7] Christiane Guguen-Guillouzo

[8] Anne Corlu

DMD Fast Forward. Published on July 21, 2011 as DOI: 10.1124/dmd.110.036848
This article has not been copyedited and formatted. The final version may differ from this version.

Legends for figures

Figure 1. The different steps of the differentiation process in HepaRG cell.

Phase contrast micrographs of HepaRG cells at proliferation stage, step 1, (A), at confluence, step 2, (B), prior DMSO addition, step 3, (C) and after 2 weeks exposure to 2% DMSO, step 4, (D). Albumin (E) and CYP3A4 (F) immunolocalization in hepatocyte colonies at step 4. Black arrows indicate the staining of interest in hepatocyte cords. BC: Biliary cells, H: hepatocytes Bar: 100 µm. Aldolase B, CYP3A4, HNF4α and C/EBPα mRNA expressions measured by northern blot during the different steps of differentiation (G).

Figure 2. Analysis of CYP4F3 expression in microsomes from differentiated HepaRG and human liver and comparison with hepatoma cell lines.

(A) Detection of CYP4F3 was performed by western blot analysis on human liver microsomes (5 µg protein), human recombinant CYP4F3B in insect microsomes (1 µg) and HepaRG microsomes (5 µg). (B) Densitometric measurement in arbitrary units of the immunoblot analysis described above. (C) CYP4F3 and CYP4A11 gene expression were quantified by qPCR in differentiated HepaRG cells and in three differentiated human hepatoma cell lines: HepG2 and HepG2/C3A, a derived clone of HepG2, collected after three weeks of culture, and Huh-7 harvested after one week of culture. Results are expressed as fold induction over HepaRG cells set at one and represent the means ± SD of two independent experiments in triplicate. (D) Total proteins extracted from HepaRG cells at different stage of differentiation were subjected to western blot analysis for CYP4F3B and CYP4A11 detection. Hsc70 was used as a loading control. (E) Differentiated cells maintained 3 days without DMSO were exposed for 24 hours to 50 µM, 100 µM or 200 µM of linoleic acid (C18:2, ω-6) or 1% BSA (control) used as lipid vehicle. HNF4α, CYP4F3B, CYP3A4, mRNA expressions were quantified by RT-PCR. Results are expressed as fold induction over vehicle-treated cells, set at one. *$p<0.05$ when compared to untreated cells and represent the means ± SD of three independent experiments in duplicate

DMD Fast Forward. Published on July 21, 2011 as DOI: 10.1124/dmd.110.036848
This article has not been copyedited and formatted. The final version may differ from this version.

Figure 3. Representative reversed-phase HPLC analysis of the metabolites generated by HepaRG cells incubated with [1-^{14}C]9(10)-EpSTA.

HepaRG cells were incubated with [1-^{14}C]9(10)-EpSTA 20 µM for 30 min at 37°C. The culture medium and cell pellets were collected separately. Radioactivity detection of compounds present (A) in the culture medium; (B) in the culture medium subjected to hydrolysis by helixpomacia suc; (C) in the cell pellet and (D) in the cell pellet subjected to hydrolysis by helixpomacia suc. RP-HPLC analysis of the radiolabeled metabolites generated by HepaRG microsomes (E) and human liver (F) microsomes incubated with [1-^{14}C]9(10)-EpSTA 75µM for 20 min at 37°C. Peak 1: glucuronoconjugates; Peak 2: 9,10-dihydroxystearic acid; Peak 3: residual substrate; Peak 4: 9,10,18-trihydroxystearic acid; Peak 5: 18-hydroxy-9(10)-epoxystearic acid, Peak 6: 17-hydroxy-9(10)-epoxystearic acid.

Figure 4. mRNA expression of ω-hydroxylase in differentiated HepaRG cells exposed to different saturated and polyunsaturated fatty acids.

Cells were treated for 6, 15 or 24 hours with 50 µM, 100 µM or 200 µM of either palmitic acid (C16:0), stearic acid (C18:0), oleic acid (C18:1, ω-9), linoleic acid (C18:2, ω-6), combination of palmitic/oleic acids or 1% BSA (control) used as lipid vehicle. CYP4F3B, CYP4A11, CYP4F2 and CYP4F12 mRNA expressions were quantified by qPCR. Results are expressed as fold induction over vehicle-treated cells, set at one and represent the means ± SD of two independent experiments in triplicate.

Figure 5. Lipid accumulation in differentiated HepaRG cells exposed to different mono and polyunsaturated fatty acids.

Phase contrast micrographs (A, C, E, G, I, K, M) and Oil-red O staining (B, D, F, H, J, L, N) of cells exposed for 24 hours to 100 µM of either oleic acid (C18:1, ω-9), linoleic acid (C18:2, ω-6), alpha-linolenic acid (C18:3, ω-3), eicosapentaenoic acid (EPA, C20:5, ω-3), docosahexaenoic

acid (DHA, C22:6, ω-3), arachidonic acid (AA, C20:4, ω-6) or 1% BSA (control) used as lipid vehicle. Bar: 50µm

Figure 6. mRNA expression of lipogenic and glucogenic genes in differentiated HepaRG cells exposed to different mono and polyunsaturated fatty acids.

Cells were treated for 24 hours with 100 µM of either oleic acid (C18:1, ω-9), linoleic acid (C18:2, ω-6), alpha-linolenic acid (C18:3, ω-3), eicosapentaenoic acid (EPA, C20:5, ω-3), docosahexaenoic acid (DHA, C22:6, ω-3), arachidonic acid (AA, C20:4, ω-6) or 1% BSA (control) used as lipid vehicle. SREBP-1c, FAS, PPARα, PPARγ, PEPCK-1, aldolase B, haptoglobin and CYP4F3B mRNA expressions were quantified by qPCR. Results are expressed as fold induction over vehicle-treated cells, set at one and represent the means ± SD of three independent experiments in duplicate *$p<0.05$ when compared to untreated cells

DMD Fast Forward. Published on July 21, 2011 as DOI: 10.1124/dmd.110.036848
This article has not been copyedited and formatted. The final version may differ from this version.

TABLE 1

Primer sequences used for RT-qPCR

RefSeq	Genes	Forward Primer	Reverse primer
NM_000896	CYP 4F3	ATTGGTTCTTGGGTCACCTG	GATGTAGGTGGGGTGGAAGA
	CYP 4F3A	ATTGGTTCTTGGGTCACCTG	CCACCAGCAGCACATATCAC (Exon 4)
	CYP 4F3B	ATTGGTTCTTGGGTCACCTG	TGATGACAGACCGGATGATG (Exon 3)
NM_017460	CYP3A4	CTTCATCCAATGGACTGCATAAAT	TCCCAAGTATAACACTCTACACAGACAA
NM_001082	CYP4F2	CACCATGAGATCCTCCTGCATATT	TCTTCCCGTCTTCATCCTTG
NM_021187	CYP4F11	ATACCACCTTGCAAAGCACC	TGGGTGGGTAGGACAGTCACT
NM_023944	CYP4F12	GCTGCCATTGCACCCAAGGATAAT	ACAGAAAGTCCATGTGCTGGAGGA
NM_000035	ALDOB	GCATCTGTCAGCAGAATGGA	TAGACAGCAGCCAGGACCTT
NM_178849	HNF4A	CAGATGATCGAGCAGATCCA	CGTTGGTTCCCATATGTTCC
NM_004364	CEBPA	AACCTTGTGCCTTGGAAATG	CCCTATGTTTCCACCCCTTT
NM_005036	PPARA	CATTACGGAGTCCACGCGT	ACCAGCTTGAGTCGAATCGTT
NM_138711	PPARG	GATGACAGCGACTTGGCAA	CTTCAATGGGCTTCACATTCA
NM_004176	SREBP-1c	TGACTTCCCTGGCCTATTTG-3	TTCAATGGAGTGGGTGCAG-3
NM_004104	FAS	GATCTCAGGGTTGGGGCTAT	TGGCCAAGGTGCTGCTGTCCCTGGA
NM_005143	Haptoglobin	CGGTTCGCTACCAGTGTAAGAAC	CCACTGCTTCTTATCATTTAAGGTGTA
NM_002046	GAPDH	GGCATGGACTGTGGTCATGAG	CATACCAGGAAATGAGCTTG

DMD Fast Forward. Published on July 21, 2011 as DOI: 10.1124/dmd.110.036848
This article has not been copyedited and formatted. The final version may differ from this version.

TABLE 2

Quantification of CYP4F3 gene expression by qPCR during the different steps of HepaRG differentiation process.

Steps of differentiation	Days of culture	CYP4F3	Aldolase B	CYP3A4	HNF4α	C/EBPα
Step 1	2	1	1	1	1	1
Step 2	10	2.26 ± 0.16	5.82 ± 1.71	1.14 ± 0.1	3.77 ± 0.57	1.03 ± 0.01
Step3	15	4.54 ± 0.36	7.72 ± 1.98	2.47 ± 0.27	6.4 ± 1.68	1.02 ± 0.01
Step 4	25	14.07 ± 1.23	13.13 ± 1.43	47.78 ± 2.09	11.26 ± 3.09	0.97 ± 0.01

Representative cell cultures of the 4 steps of the differentiation process were collected. Gene expression was quantified by real-time qPCR. Results are expressed as fold induction over day 2 of culture, set at one and represent the means ± SD of two independent experiments performed in triplicate.

DMD Fast Forward. Published on July 21, 2011 as DOI: 10.1124/dmd.110.036848
This article has not been copyedited and formatted. The final version may differ from this version.

TABLE 3

CYP4F3A and CYP4F3B mRNA quantifications in HepaRG cells, human liver tissues and human peripheral blood mononuclear cells (PBMC).

	CYP4F3B	CYP4F3A
PBMC	1	1
HepaRG cells	256	0.2
Human liver	792	0.8

qPCR analysis of total RNA extracted from differentiated HepaRG cells (day 30), human peripheral blood mononuclear cells (PBMC) and human liver tissues were performed using SYBR Green. Specific reverse primers sequences of CYP4F3A and CYP4F3B were used. Results are expressed as fold induction over PBMC, set at one for both CYP4F3 isoforms. Noteworthy, CYP4F3A expression is higher than CYP4F3B expression in PBMC. Indeed, the Ct values are 26.7 CYP4F3A and 29 for CYP4F3B in PBMC. In contrast they are 27.4 for CYP4F3A and 19.2 for CYP4F3B in differentiated HepaRG cells 27.8 for CYP4F3A and 20.2 for CYP4F3B in human liver. Results are expressed as mean obtained from two human liver samples and PBMC.

DMD Fast Forward. Published on July 21, 2011 as DOI: 10.1124/dmd.110.036848
This article has not been copyedited and formatted. The final version may differ from this version.

TABLE 4

CYP4F3B, CYP4A11, PPARα, PPARγ and SREBP-1c mRNA expressions during the HepaRG cells differentiation process

Steps of differentiation	Days of culture	CYP4F3B	CYP4A11	PPARα	PPARγ	SREBP-1c
Step 1	1	1	1	1	1	1
	2	0.82 ± 0.02	0.48 ± 0.18	1.27 ± 0.34	1.11 ± 0.005	0.63 ± 0.05
	4	0.61 ± 0.04	4.28 ± 0.51	2.06 ± 0.07	1.43 ± 0.56	0.85 ± 0.002
Step 2	10	1.85 ± 0.16	14.48 ± 2.02	6.05 ± 1.16	2.36 ± 0.76	1.16 ± 0.11
Step 3	15	3.72 ± 0.36	13.28 ± 5.94	8.14 ± 0.22	1.29 ± 1.09	1.22 ± 0.45
Step 4	25	11.54 ± 1.23	5.81 ± 2.22	13.53 ± 0.49	0.75 ± 0.56	0.89 ± 0.37

Representative cell cultures of the 4 steps of differentiation were collected. Gene expression was quantified by qPCR. Results are expressed as fold induction over the first day of culture, set at one and represent the means ± SD of two independent experiments performed in triplicate. The Ct values of HepaRG at day 25 cultured in presence of DMSO for 10 days are: 23.2 for CYP4F3, 24.55 for CYP4A11, 25.08 for PPARα, 25.61 for PPARγ and 24.03 for SREBP-1c.

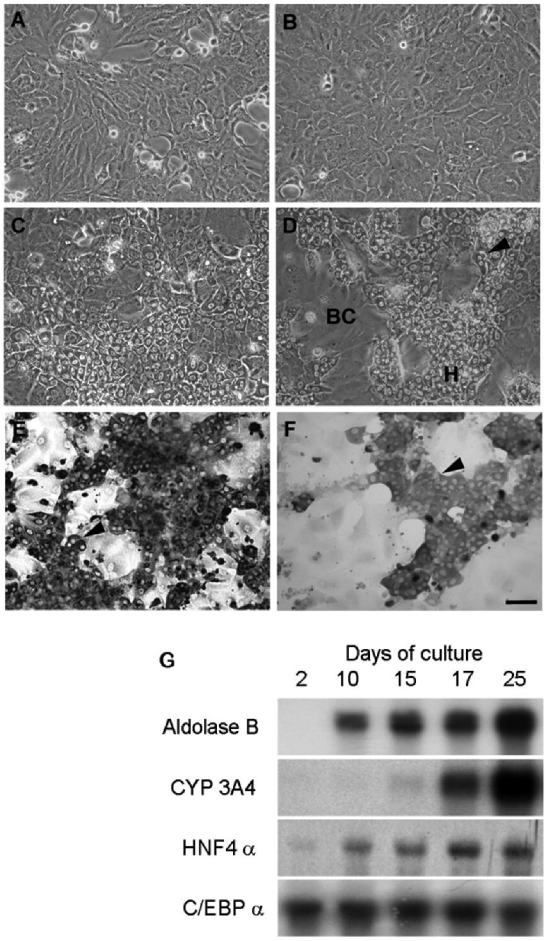
A
B
C
D
BC
H
E
F
G
Days of culture
2
10
15
17
25
Aldolase B
CYP 3A4
HNF4 α
C/EBP α

Figure 1

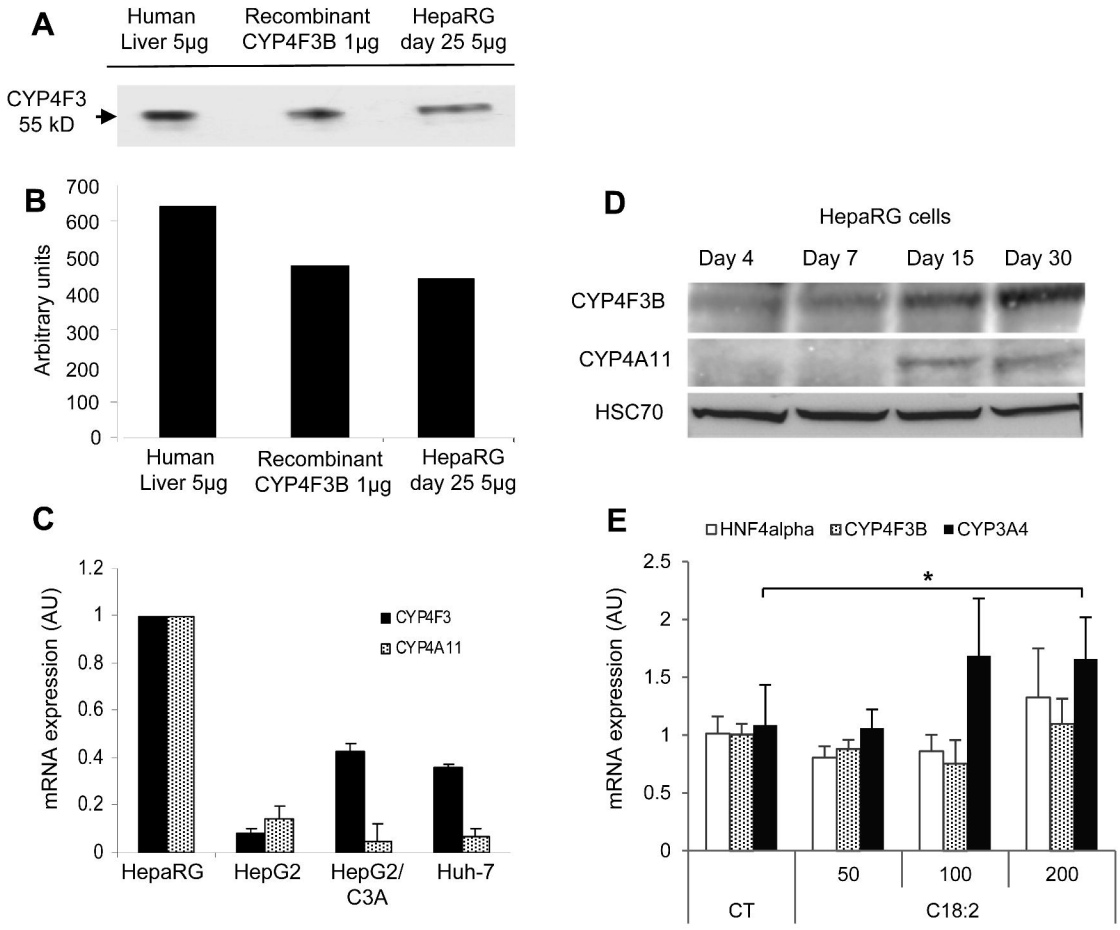
A
Human Liver 5µg
Recombinant CYP4F3B 1µg
HepaRG day 25 5µg
CYP4F3 55 kD
B
Arbitrary units
700
600
500
400
300
200
100
0
Human Liver 5µg
Recombinant CYP4F3B 1µg
HepaRG day 25 5µg
C
mRNA expression (AU)
1.2
1
0.8
0.6
0.4
0.2
0
CYP4F3
CYP4A11
HepaRG
HepG2
HepG2/ C3A
Huh-7
D
HepaRG cells
Day 4
Day 7
Day 15
Day 30
CYP4F3B
CYP4A11
HSC70
E
HNF4alpha
CYP4F3B
CYP3A4
mRNA expression (AU)
2.5
2
1.5
1
0.5
0
*
CT
50
100
200
C18:2

Figure 2

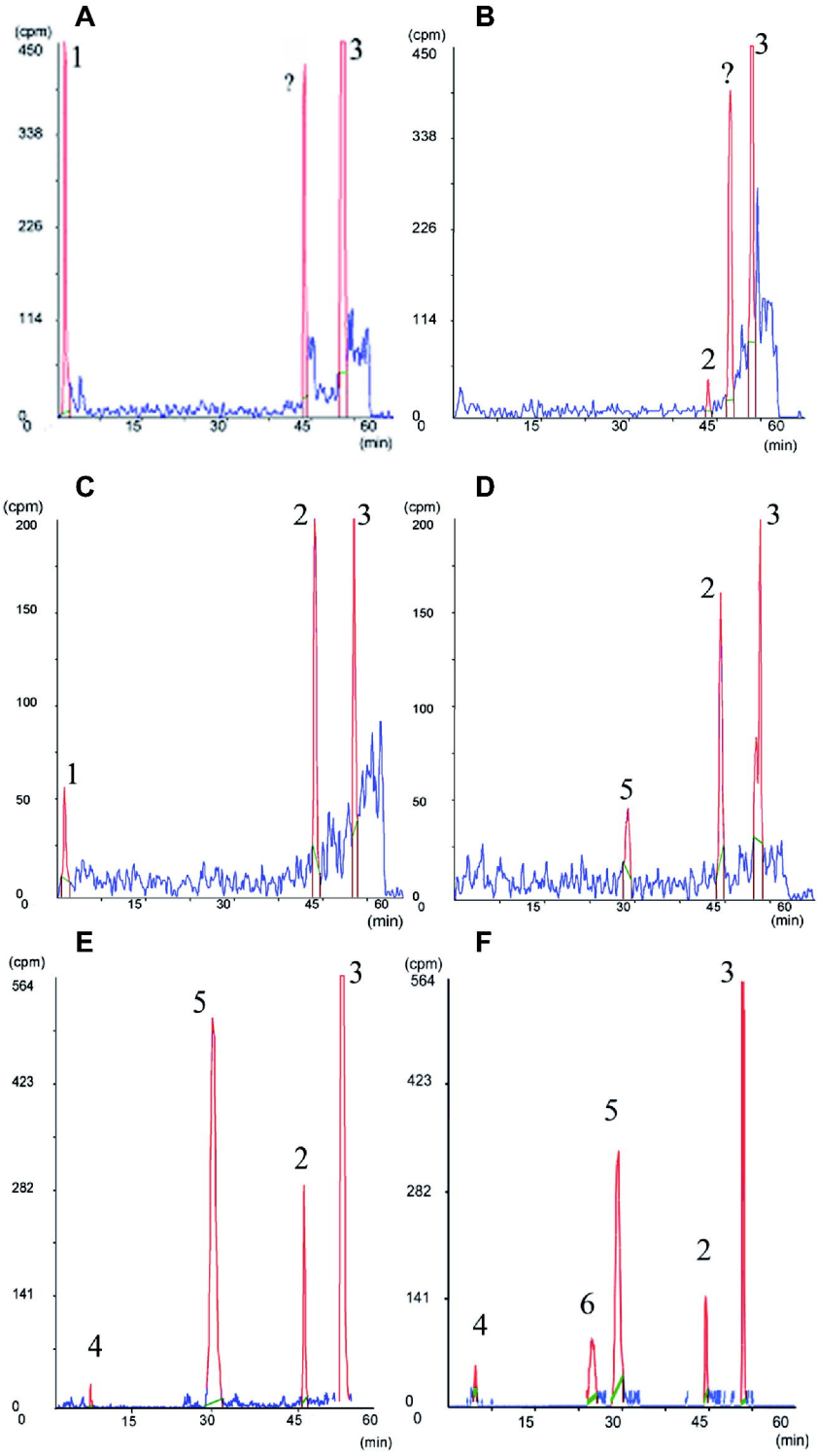
A
(cpm)
450
338
226
114
0
1
?
3
15
30
45
60
(min)
B
(cpm)
450
338
226
114
0
?
3
2
15
30
45
60
(min)
C
(cpm)
200
150
100
50
0
2
3
1
15
30
45
60
(min)
D
(cpm)
200
150
100
50
0
3
2
5
15
30
45
60
(min)
E
(cpm)
564
423
282
141
0
3
5
2
4
15
30
45
60
(min)
F
(cpm)
564
423
282
141
0
3
5
2
6
4
15
30
45
60
(min)

Figure 3

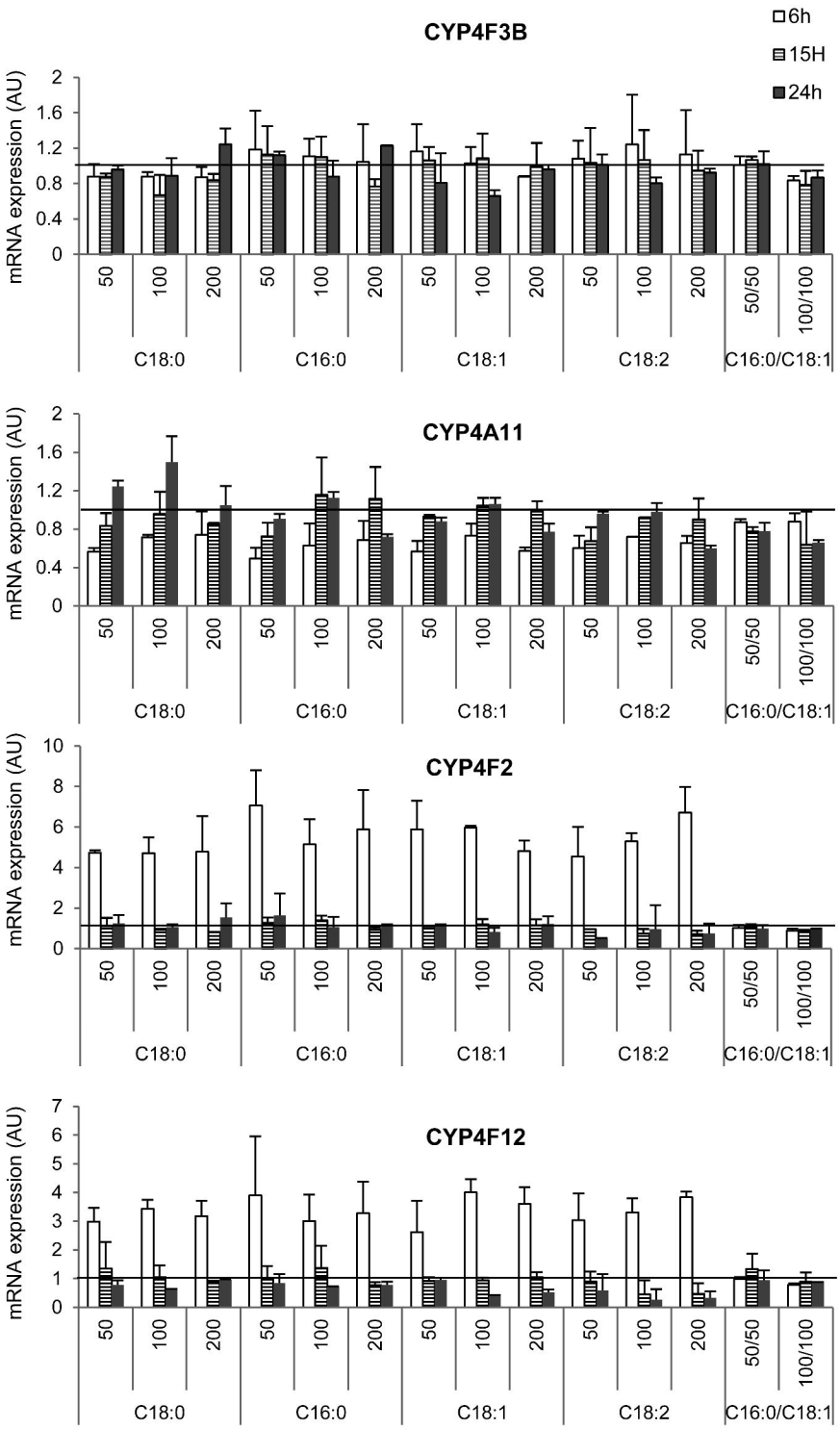
CYP4F3B
6h
15H
24h
mRNA expression (AU)
2
1.6
1.2
0.8
0.4
0
50
100
200
50/50
100/100
C18:0
C16:0
C18:1
C18:2
C16:0/C18:1
CYP4A11
CYP4F2
10
8
6
4
CYP4F12
7
5
3
1

Figure 4

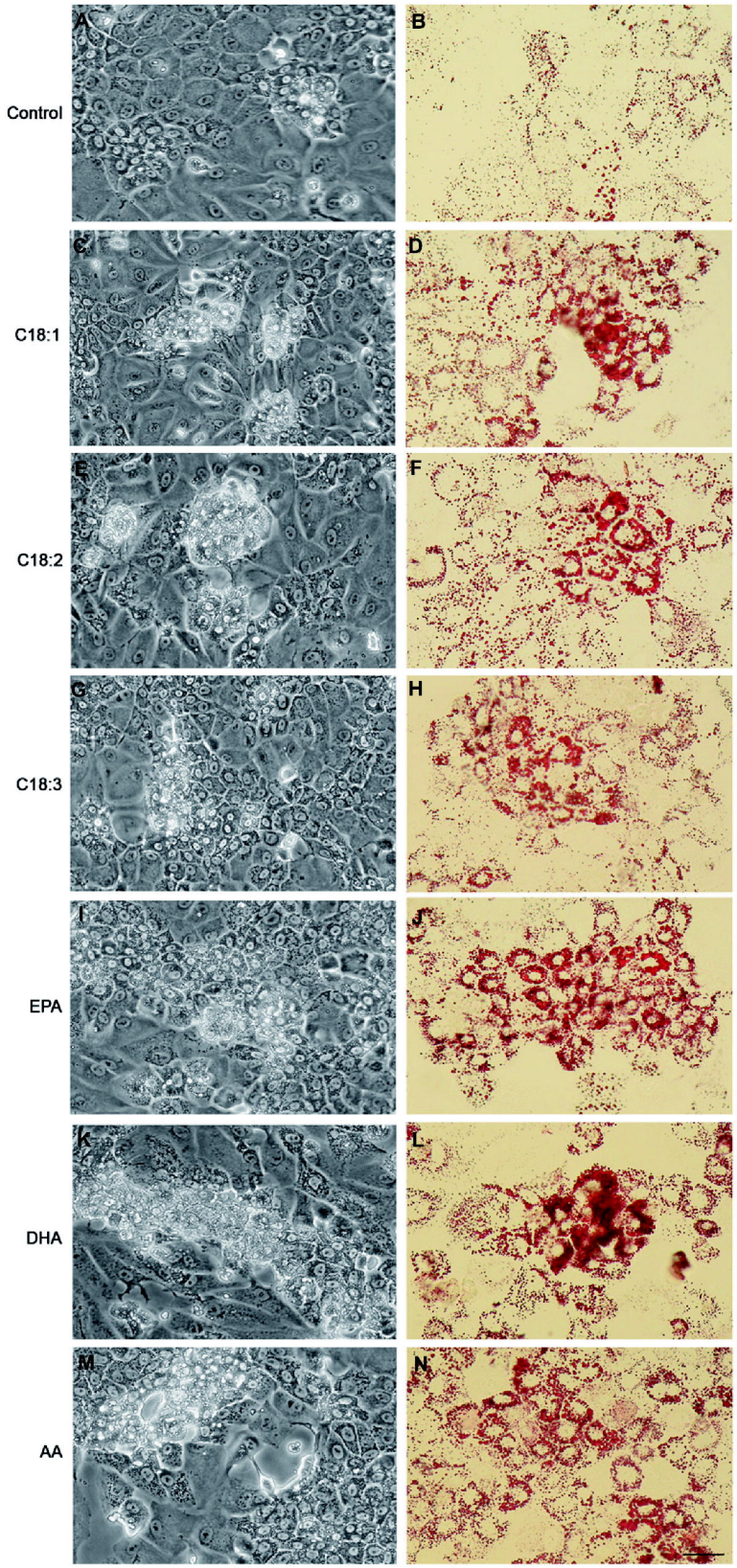

Figure 5

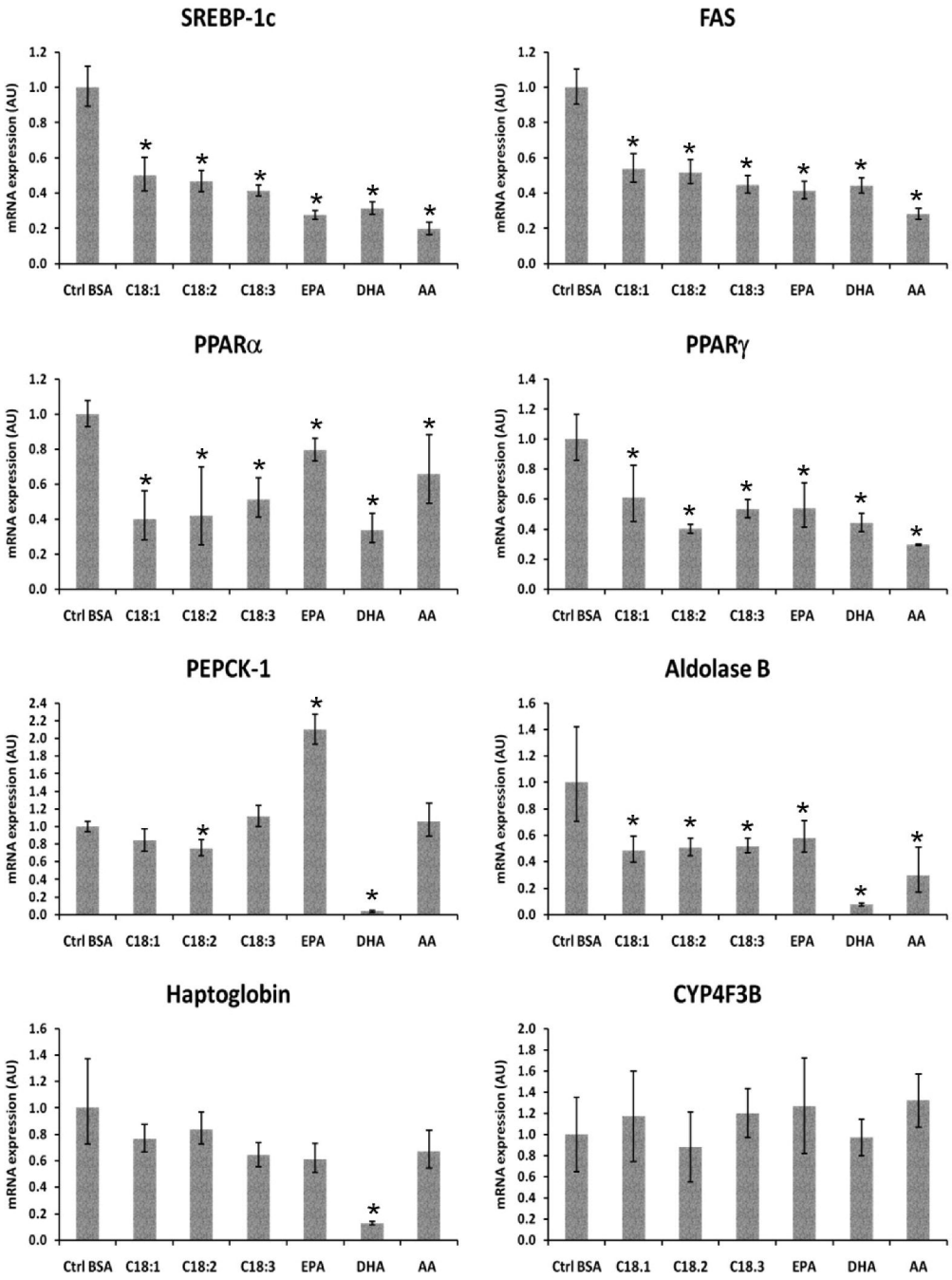
SREBP-1c
FAS
PPARα
PPARγ
PEPCK-1
Aldolase B
Haptoglobin
CYP4F3B
mRNA expression (AU)
Ctrl BSA
C18:1
C18:2
C18:3
EPA
DHA
AA
C18.1
C18.2
C18.3

Figure 6